Journal of Power Sources 228 (2013) 300–307

Contents lists available at SciVerse ScienceDirect

Journal of Power Sources

journal homepage: www.elsevier.com/locate/jpowsour

Phosphorylated polyvinyl alcohol membranes for redox Fe^{3+}/H_2 flow cells

Victor Pupkevich*, Vassili Glibin, Dimitre Karamanev

Department of Chemical and Biochemical Engineering, Western University, London, ON N6A5B9, Canada

HIGHLIGHTS

- A novel method for preparation of phosphorylated PVA membranes developed.
- A pathway of PVA phosphorylation with formation of P–C bonds suggested based on IR-spectra.
- A mechanism of proton transport within phosphorylated PVA membrane suggested.
- The membrane allowed to obtain power density of 71 mW cm^{-2} at 200 mA cm^{-2} in a Fe^{3+}/H_2 redox fuel cell.

ARTICLE INFO

Article history:
Received 21 September 2012
Received in revised form
15 November 2012
Accepted 21 November 2012
Available online 28 November 2012

Keywords:
Phosphorylation
Polyvinyl alcohol based membrane
Intrinsic proton conductivity
Transport properties

ABSTRACT

A novel method for preparation of phosphorylated polyvinyl alcohol (p-PVA) membranes was developed and used to synthesize a series of membranes with different degree of phosphorylation (4–9 wt % of phosphorus). The optimal mass ratio of PVA:H_3PO_2 was found to be 4.0:1.0, while the optimal curing time was 3 h at a temperature of 120 °C. The membranes possessed good mechanical robustness and chemical stability in acidic media. The possible pathway of PVA phosphorylation leading to formation of P–C bonds was suggested based on IR-spectra of the membranes. The water flux (6.08×10^{-2} g cm^{-2} h^{-1}) and permeability of ferric ions (3.5×10^{-5} cm^2 min^{-1}) were comparable to those of commercial Nafion 117 membrane. The dependence of the proton conductivity on the concentration of H_2SO_4 at 22 °C was studied that allowed us to predict the intrinsic proton conductivity of the p-PVA membrane (5.5×10^{-3} S cm^{-1}). The partial charges on oxygen atoms in the proposed structural units were calculated and the results permitted to suggest a mechanism of proton transport. The performance of the p-PVA membrane was tested in a Fe^{3+}/H_2 redox fuel cell showing power density of 71 mW cm^{-2} at 200 mA cm^{-2}.

1. Introduction

For over 30 years fossil fuels such as oil and coal, and their derivatives have dominated the global energy market. Today more than ever before, a heavy dependence on those resources poses a serious threat to our energy security as well as the environment. Unprecedented environmental issues associated with a very intensive and inefficient use of fossil fuels made the international community look for alternative renewable energy sources. The most abundant and sustainable ones are considered to be solar and wind power. However, successful incorporation of these sources into an existing infrastructure is quite challenging due to the necessity of using efficient means for energy storage. Nowadays, electrochemical energy conversion/storage technologies, such as fuel cells and redox flow batteries [1–4], are believed to be capable of fulfilling these requirements. The most recent and very promising amongst those is a hybrid Fe^{3+}/H_2 redox flow system discovered by Karamanev et al. [5]. It is a hybrid between a fuel cell and redox flow cell, where ferric iron gets reduced at the cathode and a hydrogen gas gets oxidized at the anode. Similar to the conventional technologies, the anodic and cathodic compartments of the cell are separated with an ion exchange membrane, which has to meet a number of requirements, such as mechanical robustness, proton conductivity, resistance to electrolytes cross-over as well as inexpensiveness [6,7], to make the technology efficient and economically feasible. For this very reason, a membrane needs to be tailored for every specific application to have a required set of properties.

The polyvinyl alcohol (PVA)-based membranes are believed to be promising components for the direct methanol fuel cells (DMFC) [8–14], hydrogen-oxygen fuel cells [9,15], direct borohydride fuel cells [16] and other applications [17] mainly due to their low cost and

* Corresponding author. Tel.: +1 519 661 2111x88237; fax: +1 519 661 3498.
E-mail address: vpupkev@uwo.ca (V. Pupkevich).

0378-7753/$ – see front matter © 2012 Elsevier B.V. All rights reserved.
http://dx.doi.org/10.1016/j.jpowsour.2012.11.080

good oxidative and hydrolytic stability. Since PVA membranes do not have high proton conductivity, various methods are used to improve proton conductive functionality, such as blending with sulfonated phenolic resins [8], poly(styrene sulfonic acid) [9], poly(acrylo-2-methyl-1-propanesulfonic acid) [10,11], poly(styrene sulphonic acid-co-maleic anhydride) [12]; the use of PVA esterification by chloro-sulfonic acid [13], aliphatic or aromatic disulfo-acids [14,15], phosphoric acid [18,19] as well as sol–gel method [20,21]. To prevent the leaching out of water soluble substances with acidic functionality, the cross-linking is often required. It is usually done by dialdehyde cross-linking [7,11,13,15] or by using esterification reactions [13–15,17]. The sulfoacids-based membranes serve as superior methanol barriers and show proton conductivity comparable to or better than that for Nafion membranes [8–15]. However, such membranes demonstrate good conductivity at high humidity only. The blends of PVA with compounds bearing phosphonate or phosphate functional groups, as well as phosphorylated PVA (p-PVA), demonstrate the ability to retain the water of hydration in the temperature range of 80–125 °C and relatively high proton conductivity at low humidity [19,22]. Different methods are used for the phosphorylation of PVA [18,19]. Those include, along with using phosphoric acid or $POCl_3$, the application of auxiliary compounds and demand complex techniques of synthesis. The aim of this work was to develop a novel method of the PVA membranes phosphorylation using hypophosphorous acid and to study their transport properties as well as performance in an actual hybrid Fe^{3+}/H_2 redox flow cell.

2. Experimental

2.1. Materials

Polyvinyl alcohol (Elvanol® 71-30 by DuPont, Germany) was used as received. The 0.5 M hypophosphorous acid (H_3PO_2) solution was obtained from $NaHPO_2 \cdot H_2O$ (Sigma–Aldrich, USA) by an ion exchange method [23] using cation exchange resin Dowex® HCR-W2, grade 16-40 (J.T. Baker Chemical, USA) in H^+ form. The hydrogen gas diffusion electrode ELAT® LT 140 EW (BASF, USA) and the proton exchange membrane Nafion® 117 were purchased from the Fuel Cell Store (USA). The Selemion HSF ion exchange membrane was obtained from Asahi Glass Corporation (Japan). Ammonium heptamolybdate tetrahydrate ($(NH_4)_4Mo_7O_{24} \cdot 4H_2O$) and ammonium metavanadate (NH_4VO_3) were purchased from J.T. Baker Chemicals (USA).

2.2. Phosphorylation of the PVA

Polyvinyl alcohol was dissolved in deionized (DI) water by stirring at 90 °C to obtain a 5% (w/w) solution. Then, a series of PVA solutions with H_3PO_2:PVA mass ratios in the range of 6.0:1.0 to 1.5:1.0 were prepared by mixing aqueous solutions of 0.5 M H_3PO_2 and 5% PVA. After rigorous stirring of the mixtures at room temperature for 30 min, the solutions were degassed under vacuum, cast into molds (polystyrene Petri dishes) and kept at 40 °C for 3 days to obtain the films. The hardened films were separated from the molds and heat-treated at given temperature and time of curing. The obtained phosphorylated PVA films had a slightly yellowish colour and were flexible, mechanically robust and insoluble in water. The films readily swelled in water and different electrolyte solutions, forming transparent gel membranes with good mechanical properties. Before characterization, the membranes were washed in DI water to get rid of un-reacted phosphoric acids until pH was 5.0 in the washing water. The thickness of the membranes synthesized was in the range 0.15–0.30 mm. To estimate their hydrolytic stability, some membranes were kept in 2 M H_2SO_4 at ambient temperature for about one year and their appearance and mechanical robustness were qualitatively tested.

2.3. Experimental techniques

2.3.1. FT-IR spectra measurement

FT-IR spectra of the membranes were measured using a Bruker IFS55 FTIR spectrometer equipped with Attenuated Total Reflection (ATR) attachment with germanium crystal.

2.3.2. Spectrophotometry

The spectrophotometric method reported by Banks et al. [24] was used to determine the content of phosphorus introduced into the membranes during phosphorylation. The specimens of ~10 mg were completely hydrolysed by boiling in concentrated nitric acid to form phosphoric acid. Further, a mixture of ammonium metavanadate and ammonium molybdate was added to the solution diluted by 50% nitric acid, after 30 min, the absorbance at 400 nm was measured using Varian Cary 5 spectrophotometer. The amount of phosphorus was determined from the calibration curve obtained for a series of KH_2PO_4 solutions.

2.3.3. Swelling

Swelling properties of the phosphorylated PVA membranes were estimated by determination of the water uptake and changes in dimensions. To determine their water uptake, membrane samples of 0.2–0.3 g were immersed in DI water at 22 °C for 24 h, and then weighed and dried at 105 °C until a constant weight was reached. Before weighing, surface water was wiped off with filter paper. The water uptake (W, %) was calculated as a ratio of the weight difference between swollen and dry specimens to the weight of a dry specimen. The length change (Δl, %) was evaluated by measuring the lengths of a membrane specimen swollen in water at 22 °C and that of dry one using the following formula:

$$\Delta l = \frac{l_s - l_d}{l_d} \times 100 \quad (1)$$

where l_s and l_d are the lengths of a swollen and dry membrane, respectively.

2.3.4. Proton conductivity

The proton conductivity of p-PVA gel membranes was measured in a series of sulphuric acid solutions (0.05–2.00 M H_2SO_4) at 22 °C by a two-probe direct current potentiometric method using an electrodialysis cell consisting of five compartments, as described by Pupkevich et al. [25] and Balgobin et al. [26]. The voltage drop (u, mV) across the membrane as a function of the applied current was measured by a pH-meter/mV-meter Orion 420A. The current was gradually increased while the potential drop was recorded. The slope of the u–i plots (Fig. 1) gave the area resistance of the membrane. Prior to measurements, the membranes were equilibrated with the sulphuric acid solution for 12 h. Proton conductivity was calculated using the following equation:

$$\sigma = L/R \quad (2)$$

where σ is the proton conductivity (S cm^{-1}), L is the thickness (cm) of the p-PVA membrane, and R is the area resistance (Ohm cm^2).

2.3.5. Ferric ion permeability

The permeability of ferric ions through the p-PVA gel membrane and Nafion 117 membrane was estimated by electro-dialysis in the setup used for measuring membranes resistance [25]. The anodic compartment was filled with the solution of 0.45 M $Fe_2(SO_4)_3$ in 1 M

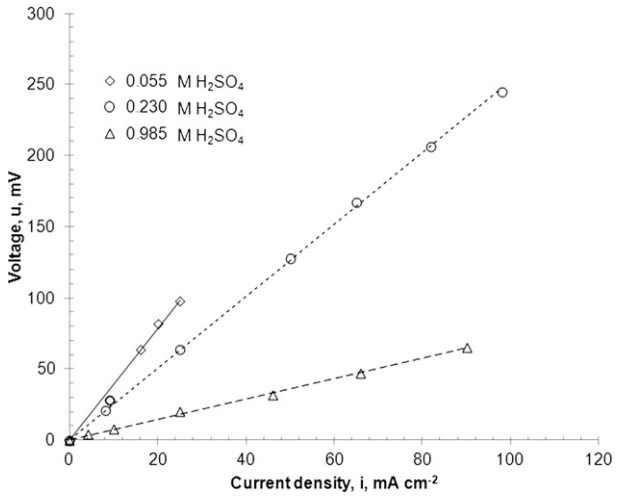

Fig. 1. The dependence of a voltage drop across the synthesized p-PVA membrane on applied current at different concentrations of H_2SO_4.

H_2SO_4 and the cathodic compartment was filled with 1 M H_2SO_4. The volume of each reservoir was 100 mL. The applied current, the electro-dialysis time and membranes surface area were 0.25 A, 7 h and 12.3 cm^2, respectively. It was established that the change in ferric iron concentration in the anodic compartment is negligible during the electro-dialysis experiments, i.e. a pseudo-steady-state condition within the membrane was established. The permeability of ferric ions was calculated by the following equation [27]:

$$p = \frac{V_c[\mathrm{d}C_c(t)/\mathrm{d}t]L}{A(C_a - C_c)} \quad (3)$$

where p is the permeability of ferric ions ($cm^2\ min^{-1}$), V_c, L and A are the volume of cathodic compartment (mL), the thickness (cm) and the area of the membrane (cm^2), respectively. C_a and C_c are the concentration (mol L^{-1}) of ferric ions in anodic and cathodic compartments, respectively, and $dC_c(t)/dt$ refers to the ferric ion concentration in the cathodic compartment as function of the time.

2.3.6. Water flux

The water flux was estimated at 22 °C using a gravimetric method (Fig. 2). The water flux is a very serious constrain for the Fe^{3+}/H_2 fuel cell [5] due to the possibility of flooding of the hydrogen diffusion electrode. To measure it, the p-PVA membrane

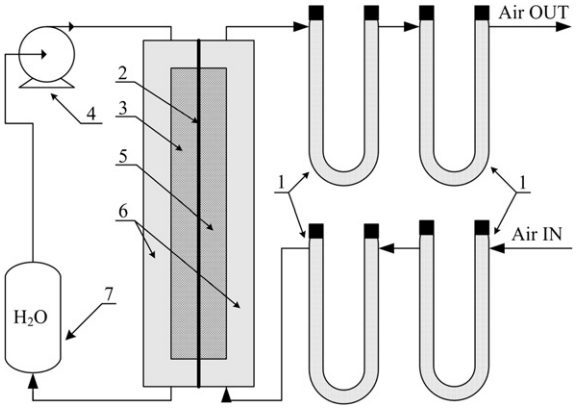

Fig. 2. The setup for water flux determination. 1 – U-tubes filled with granulated KOH, 2 – membrane under study, 3 – graphite felt cathode, 4 – pump, 5 – gas diffusion hydrogen electrode, 6 – flow distribution plates, 7 – reservoir.

was sandwiched between a graphite felt electrode and a hydrogen diffusion electrode in a 4 × 4 cm cell with serpentine flow distribution channels that were similar to these in the above-mentioned fuel cell. Water was circulated through the graphite felt, and dry air was passed through channels on the gas diffusion electrode side. The water vapour carried out of the cell by air was absorbed by two consecutively connected U-tubes filled with granulated KOH. In order to make sure that the incoming air is absolutely dry, two U-tubes with an absorbent (KOH) were put right before an inlet of the measuring cell. For comparison, the same test was performed for a commercial Nafion-117 membrane. Water flux was calculated by the following equation:

$$F_w = \frac{m_t - m_0}{A \cdot t} \quad (4)$$

where F_w is the water flux through the membrane ($g\ cm^{-2}\ h^{-1}$), m_t and m_0 are the weights of U-tubes with an absorbent after and before the experiment (g), respectively, t is the time of the experiment. The membrane thickness was 0.25 mm in all cases.

2.3.7. Performance testing

In order to find out the electrochemical performance of the synthesized p-PVA membranes (and Selemion HSF membrane for comparison) were tested in the Fe^{3+}/H_2 fuel cell. The membrane under investigation was sandwiched between the activated graphite felt (cathode) and hydrogen gas diffusion electrode (anode), and 0.45 M solution of $Fe_2(SO_4)_3$ in 1 M H_2SO_4 was pumped through the cathodic chamber and hydrogen was supplied to the anode [28]. The steady-state polarization curves were recorded for a fuel cell operated under hydrogen pressure of 101.3 kPa. The activation of graphite felt was performed as described by Pupkevich et al. [28].

3. Results and discussion

3.1. Synthesis and physico-chemical properties of p-PVA gel membranes

It was previously mentioned that the p-PVA membranes transform into gel membranes after swelling in water or electrolyte solutions. A series of experiments was performed in order to investigate the influence of the temperature, mass ratio PVA:H_3PO_2 (hereafter will be referred as ratio) and time of curing on the properties of p-PVA membranes. It was established that in the range of ratios from 6.0:1.0 to 1.5:1.0 the temperature and time of curing are the key factors affecting properties of the p-PVA membranes. For instance, the water uptake of the p-PVA membranes phosphorylated at 115 and 130 °C (the ratio 4.0:1.0 and time of phosphorylation 1 h) was 224 and 127%, respectively. The elongation of p-PVA membranes (the ratio 4.0:1.0 and the temperature of curing 120 °C) was observed to reduce from 31.0 to 17.5% after increasing the phosphorylation time from 1.5 to 3 h. The experiment conducted in this work showed that the ratio 4.0:1.0 and 3 h of curing time at 120 °C (the content of phosphorus was 4–5% of the dried membrane weight) allow, to a first approximation, to get the optimal set of physico-chemical properties. The proof of such a suggestion is the appearance of gel membranes and their physical properties such as size, mechanical robustness, transparency and proton conductivity, which did not change after a year of keeping in 2 M H_2SO_4 at 22 °C. Apparently, it is due to very slow hydrolysis of polyvinyl alcohol phosphate esters at ambient temperature. For this very reason kinetic studies of the hydrolysis of different organic phosphates have been conducted at elevated temperatures (~100 °C) [29]. Relatively good hydrolytic stability of these ester linkages at moderate

temperatures (20–80 °C) is favourable in terms of using p-PVA membranes in low temperature fuel cells and redox flow batteries. The water flux of the synthesized membrane was determined to be 6.08×10^{-2} g cm^{-2} h^{-1}, which is about 1.7 times larger than that for Selemion HSF membrane (3.52×10^{-2} g cm^{-2} h^{-1}). The permeability of ferric ions through the membrane was also higher (3.5×10^{-5} cm^2 min^{-1}) in comparison with Nafion 117 membrane (1.32×10^{-5} cm^2 min^{-1}). In our opinion, the larger values of water flux and ferric ions permeability through the p-PVA gel membranes could be caused by their less dense structure and higher hydrophilicity.

3.2. Interpretation of IR-spectrum of the p-PVA membrane

It is well-known that the IR spectrum of a molecule or a polymer is a so-called "fingerprint" and is usually used for the purpose of identification and, in the absence of a suitable reference database, for characterization of an unknown sample [30]. To obtain more detailed information on chemical structure of the p-PVA membrane, we compared the observed stretching frequencies (wave numbers) (Fig. 3) with those predicted for the suggested structures (Fig. 4) formed within the membrane, and for the chemical bonds in different compounds [30–42]. The structural units with pendant phosphate and phosphonate groups as well as cyclic and interconnected structural units were taken into consideration. In order to more easily estimate the stretching frequencies of chemical bonds, we used so-called "diatomic approximation" [43]. In terms of this approximation, the IR spectrum is considered to be a superposition of the stretching frequencies of an assembly of the diatomic oscillators. The wave number of the stretching motion for a pair of atoms forming a chemical bond may be found from the following equation [30,43], provided that each oscillator acts as a harmonic oscillator:

$$\nu = 1303\sqrt{k_e/\mu} \tag{5}$$

where ν is the wave number (cm^{-1}), k_e is the stretching force constant (N cm^{-1}), μ is the reduced mass ($\mu = m_i m_j/(m_i + m_j)$) of i and j atoms forming chemical bond (atomic units). This equation gives a relationship between a force constant of the covalent bond, the masses of interacting atoms and the frequency of a vibration. A

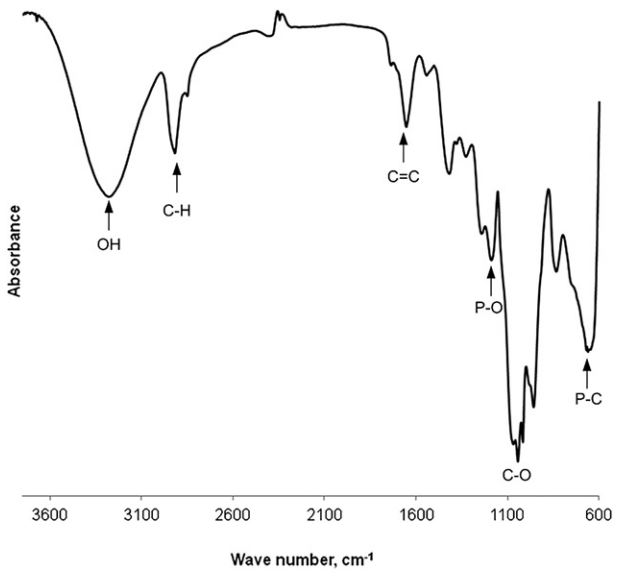

Fig. 3. FTIR spectrum of the synthesized p-PVA membrane.

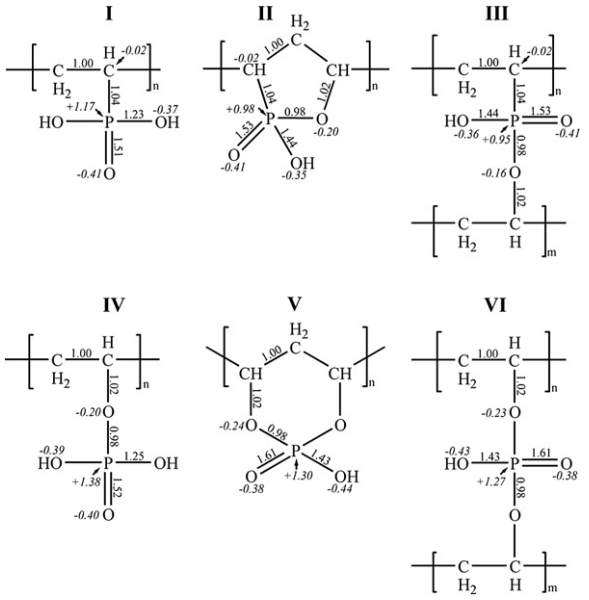

Fig. 4. The suggested structural units of the phosphorylated PVA membranes.

reasonably good fit between the bond stretching vibrations predicted by the Equation (5) and experimental values was observed. In the present study, the values of force constants were estimated using the Badger's rule [44]. A general form of the Badger's rule is expressed as follows:

$$k_e = \left[C_{ij}/(r_e - d_{ij})^3\right] \tag{6}$$

where C_{ij} and d_{ij} are the adjustable constants for a bond (Å), r_e is the equilibrium bond length (Å). The values of a constant d_{ij} were determined as the sum of d_i and d_j atomic constants [45] of the bonded atoms (Table 1), and the values of C_{ij} were considered as the fitting parameters. Using literature data [46–50] on bond lengths and force constants, the following equations were derived:

$$k_e(\mathrm{C-C}) = 2.665(r_e - 0.672)^{-3} \tag{7}$$

$$k_e(\mathrm{C-O}) = 2.624(r_e - 0.610)^{-3} \tag{8}$$

$$k_e(\mathrm{C-P}) = 1.88(r_e - 0.927)^{-3} \tag{9}$$

$$k_e(\mathrm{P-O}) = 2.07(r_e - 0.865)^{-3} \tag{10}$$

In turn, the bond lengths in the suggested structures were estimated using the Brown's rule of a bond valence sum [51], where the principle of the conservation of valency (v) associated with each atom is used. The sum of the bond valences (orders) of all the bonds formed by an atom is equal to the atomic valency. There are following relationships to determine the bond valences of C–H, C–C, C–O, C–P and P–O bonds [52,53]:

Table 1
Atomic parameters for calculation of Badger's d_{ij} constants.

Atom	d, Å	Atom	d, Å	Atom	d, Å	Atom	d, Å
H	0.094	O	0.274	S	0.567	Se	0.754
B	0.532	F	0.360	Cl	0.637	Br	0.809
C	0.336	Si	0.602	Ge	0.735	Sb	0.950
N	0.328	P	0.591	As	0.751	I	1.011

$$S_{C-C} = \exp[(1.54 - r_{C-C})/0.24] \quad (11)$$

$$S_{C-H} = \exp[(1.08 - r_{C-H})/0.23] \quad (12)$$

$$S_{C-O} = \exp[(1.43 - r_{C-O})/0.27] \quad (13)$$

$$S_{P-O} = (r_{P-O}/1.620)^{-4.29} \quad (14)$$

$$S_{C-P} = \exp[(1.87 - r_{C-P})/0.30] \quad (15)$$

where S is the bond valence (valence units), and r_{C-C}, r_{C-H}, r_{C-O}, r_{P-O}, r_{C-P} are the bond lengths (Å). If a bond valence is known, the bond length can be easily calculated by a trial-and-error method. The Equation (15) is a result of the present study based on mean values of the bond lengths [50] for single (1.84 Å), double (1.66 Å) and triple (1.53 Å) carbon–phosphorus bonds. The bond valences of C–P, C–O(P), P–O(C), C–C and C–H were taken to be $S = 1$, as a first iteration. The bond valence of the phosphoryl (P=O) group was estimated by the following formula [53]:

$$S_{P=O} = \left[0.175\ln\left(\frac{224,500\ \mathrm{cm}^{-1}}{\nu}\right)\right]^{-4.29} \quad (16)$$

A bond valence $S_{P=O}$ was calculated to be 1.5 for a hydrogen bonded phosphoryl group in diisopropyl methylphosphonate ($\nu = 1230\ \mathrm{cm}^{-1}$) [32]. Further, a difference between the valence of P atoms (5 in this particular case) and a sum of bond valences of P–O(C), P–C and P=O bonds was distributed over P–O(H) bonds. After a number of adjustments, the final schematics of bond valences distribution are shown in Fig. 4, where the bond valences are written over the bonds in plain font. The estimations of bond lengths by Equations (11)–(15) are summarized in Table 2. It can be seen that this approach gives the values of the bond lengths that are in a relatively good agreement with experimental ones. Then, the tabulated bond lengths were used to calculate the wave numbers of different bonds by Equations (5), (7)–(10). The estimated and experimentally obtained values for stretching frequencies on characteristic stretching modes of the bonds along with the literature data [30–42] are presented in Table 2. A comparison of experimental and calculated values showed that an error of the method is ±20–25 cm^{-1}. It is interesting to note, that the phosphorylation of PVA by H_3PO_2 results in the C=C bonds formation with the characteristic band at 1662 cm^{-1} (Fig. 3). This phenomenon was also observed when phosphoric acid was used [24,54] and believed to be due to the chain–stripping elimination of water from a PVA matrix with polyene formation. The intensive, broad band at 3283 cm^{-1} belongs to the stretching vibration of hydrogen bonded OH-group [30,31]. The bands at 2924 and 2855 cm^{-1} correspond to the methylene C–H asymmetric and symmetric stretching vibrations, respectively, and the band at 970 cm^{-1} was assigned to the *trans*-C–H out-of-plane bending vibrations [30,31]. The comparison of P–C vibrations in a number of compounds (Table 2) with the observed stretching vibrations at 663 and 752 (shoulder) cm^{-1} (Fig. 3) and calculated (674 cm^{-1}) by the Equations (5), (9) and (15) confirms the formation of a P–C bond. Apparently, the shoulder at 752 cm^{-1} and band at 663 cm^{-1} can be attributed to the asymmetric and symmetric vibrations of the P–C bond. The vibrations in the range of 950–1055 cm^{-1} were assigned to the stretching vibrations of P–O–C linkages in alkyl phosphate esters [31]. As indicated by Rao [31], it was not possible to specifically associate the bands at 1055-950 cm^{-1} with the stretching of either the P–O or the C–O bond.

Table 2
Bond lengths, force constants and stretching vibrations of the bonds in the suggested structures of the p-PVA membrane.

Bond	Structure	r_e, Å		k_e, N cm^{-1}	ν, cm^{-1}		
		Calculated	Literature data		Calculated	Observed (Fig. 3)	Literature data
C–O(H)	PVA	1.424	1.364 [65]	4.86	1097	1094	1095 [37]
C–O(P)	I–VI	1.435	1.425, 1.481[a] [33]	4.67	1075	1094 1047	950–1055, range for C–O-(P) linkage [31] 1070, 1025[k] [41] 1060(ν_{as}), 1047(ν_s)[a] [33]
C–P	I–III	1.86	1.863[b] [34], 1.846[c] [42] 1.773[d] [66]	2.31	674	663 752, sh	650–750, range for P–C (aliphatic) bond [40] 676[b] [34], 740[l] [39] 671, 756[f] [40]
P=O	I–III	1.469	1.47[e] [67], 1.476[f] [50]	9.39	1230	1250	1250–1350 [30] range of organic phosphates
	IV	1.467	1.457[g] [68]	9.49	1236	1250	1298[e] [35]
	V, VI	1.449	1.430[h] [48]	10.39	1293	1330	1254 [37], 1278 [36]
P–O(H)	I	1.543	1.539–1.550[d] [66]	6.64	1034	1047	1068 [38]
	II, III	1.488	1.54[e] [67]	8.56	1174	1190	–
	IV	1.538	–	6.79	1045	1047	1055 [36]
	V, VI	1.490	1.573[g] [68] –	8.48	1168	1190	–
P–O(C)	II, III	1.627	–	4.68	868	837	780–850, range for P–O–C linkage [31]
	IV–VI	1.627	1.597[i] [69], 1.626[j] [69] 1.536, 1.582[a] [33]	4.68	868	752, sh 837 752, sh	827(ν_{as}), 754(ν_s)[a] [33] 860, 760[m] [41]

[a] Ammonium dimethyl phosphate.
[b] $H_3C–PH_2$.
[c] $(CH_3)_3P$.
[d] Benzenphosphonic acid.
[e] $HPO(OH)_2$.
[f] $(CH_3)_3PO$.
[g] H_3PO_4.
[h] P_4O_{10}.
[i] Methylphosphomonoester.
[j] Propargylphosphomonoester.
[k] Tribytyl phosphate.
[l] Tetradecane phosphonic acid.
[m] Trimethylphosphate, sh – shoulder.

However, *ab initio* calculations [33] and our estimations let single out specific vibrations. The band at 837 cm^{-1} and the shoulder at 752 cm^{-1} (coupled with P–C bond vibrations) can be assigned to the asymmetric and symmetric vibrations of the P–O bond in the ester linkage, respectively. The bands at 1094 cm^{-1} (coupled with C–O(H) band of PVA backbone) and 1047 cm^{-1} are asymmetric and symmetric stretching modes of the C–O bond, respectively. It should be noted, that the calculated wave numbers for P–O(C) bonds in different structures are significantly higher than experimental values. Apparently, the real bond valence of this bond is lower than assumed (0.98), which could facilitate the cleavage of the P–O bond by the reaction of hydrolysis and, as a consequence, affect hydrolytic stability of the phosphorylated PVA products. This also explains the ability of p-PVA to dissolve in concentrated solutions of strong acids, such as HCl, H_3PO_4 and H_2SO_4. The phosphoryl group absorption occurs in the region of wave numbers of 1170–1350 cm^{-1} [32,40]. According to our calculations, the cyclization and cross-linking could affect the stretching vibrations of phosphoryl group and P–O(H) bond (Table 2). The comparison of observed bands for P=O group at 1330 cm^{-1} and the P–O(H) bond at 1190 cm^{-1} with predicted ones (Table 2) confirms the formation of the cyclic and interconnected structures. Thus, taking into account all the above-mentioned results we can conclude that phosphorylation of PVA membranes by H_3PO_2 leads to formation of the complex structure, formed by interconnected polyvinyl alcohol chains with pendant and cyclic phosphate and phosphonate groups. The interconnected diester structures provide necessary cross-linking of the PVA membranes. The formation of C=C bonds opens up the possibility to further modify the membranes functionality by various organic chemistry reactions. The following pathway of interaction between PVA and H_3PO_2 can be suggested. The reaction starts with oxidation (by air) and simultaneous disproportionation of H_3PO_2 to give H_3PO_3 and H_3PO_4:

$$2H_3PO_2 + 1.5O_2 = H_3PO_3 + H_3PO_4 \quad (17)$$

Further, some dehydration of PVA catalysed by H_3PO_4 results in the formation of C=C bonds followed by the reactions of C–P bonds formation, i.e. creation of phosphonate groups:

$$-HC{=}CH - CH - + H_3PO_3 + 0.5O_2 = - HC{=}CH - C(OH)PO(OH)_2 - \quad (18)$$

$$-HC{=}CH - CH_2 - + H_3PO_2 + 0.5O_2 = - HC - H_2C - PO(OH)_2 - CH_2 - \quad (19)$$

The schemes of the final reactions of phosphate and phosphonate esters formation are well-known [55–57] and therefore are not given here.

3.3. Partial charges on oxygen atoms

Charges on oxygen atoms (δ_i) in a molecule can be estimated in terms of the partial charge model by the following equation [58]:

$$\delta_i = (X - X_i^o)/1.36\sqrt{X_i^o} \quad (20)$$

where X is the equalized electronegativity of a molecule, X_i^o is the electronegativity of i-atom. Equalized electronegativity is a geometric mean value of the electronegativity of all atoms composing a molecule. The well-known Allred-Rochow's scale of electronegativity was used for calculation of X values [59]. In calculations of the equalized electronegativity, the structures I–VI (to maintain the electroneutrality of a structure) were terminated by $-CH_2CH(OH)CH_3$ radical. The values of equalized electronegativities of such molecules were calculated by a method proposed by Carver et al. [60]. The following values of equalized electronegativity were obtained for the structures I–VI and PVA backbone: I – 2.465, II – 2.449, III – 2.461, IV – 2.492, V – 2.537, VI – 2.534, PVA – 2.575. Using these values, the charges on atoms in different structures were calculated. The charges are presented in Fig. 4 and written in italics. It seems that the approach chosen for estimation of charges works reasonably well and allows to attain the reliable values. In particular, the charges on the P atom (as a central atom) in structures I–VI calculated by the above-mentioned model are close to those obtained by the quantum chemical calculations for vinylphosphonic acid (+1.17 [61] and +1.443 [62]). We believe that increased density of negative charges on oxygen atoms in structures I–VI results in extra hydrogen bonding within the p-PVA matrix and affects not only proton conductivity, but also water flux through the membrane and other transport properties.

3.4. Proton conductivity

The p-PVA gel membranes show relatively high proton conductivity (compared to commercial Selemion and Nafion membranes) when they are doped by sulphuric acid. It can be seen from Fig. 5 that proton conductivity is greatly affected by the concentration of sulphuric acid. This dependence at 22 °C is described by the following equation:

$$\sigma = -8.96 \times 10^{-4} C_{H^+}^3 + 5.19 \times 10^{-3} C_{H^+}^2 + 7.96 \times 10^{-3} C_{H^+} + 5.51 \times 10^{-3} \quad (21)$$

where σ is the proton conductivity (S cm^{-1}) and C_{H^+} is the concentration of hydrogen ions (mol L^{-1}).

When the concentration of H^+ ions approaches zero, the proton conductivity approaches the "intrinsic" proton conductivity, which is equal to 5.51×10^{-3} S cm^{-1} in this particular case. This value is by 2.5 orders of magnitude higher than that of a pure PVA membrane (3.65×10^{-5} S cm^{-1} [63]). We believe that such a significant difference can be explained by formation of strong acid–base complexes with sulphuric acid due to the high density of negatively charged oxygen atoms. Apparently, those complexes cannot be completely hydrolysed by water during washing and, therefore, higher intrinsic proton conductivity of the membrane is associated

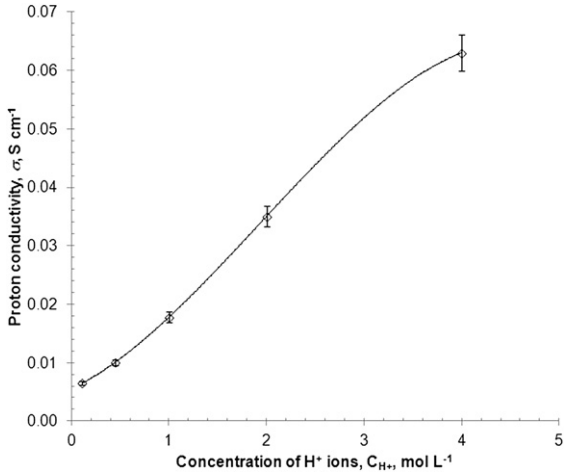

Fig. 5. The dependence of proton conductivity of the p-PVA membrane on the concentration of hydrogen ions in doping solution.

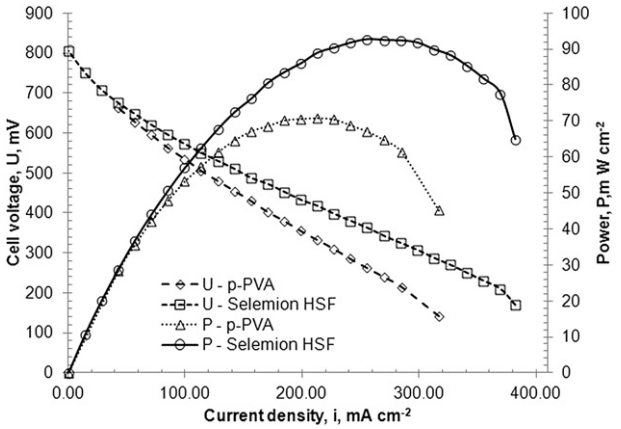

Fig. 6. Performance of p-PVA and Selemion HSF membranes in a single Fe^{3+}/H_2 redox fuel cell at 22 °C.

with participation of the "traces" of acid–base complexes in a proton transport process. However, the lower intrinsic proton conductivity in comparison with Selemion HSF and Nafion 117 membranes permits to suggest the Grotthuss mechanism [64] of proton conductivity in phosphorylated PVA gel membranes doped by "traces" of strong acids.

3.5. Testing in an actual Fe^{3+}/H_2 fuel cell

The results of the membranes testing in an actual fuel cell are presented in Fig. 6. The figure compares the power and current–voltage behaviour of a Fe^{3+}/H_2 fuel cell at ambient temperature with two different membranes: the synthesized p-PVA and Selemion HSF. As can be seen from the figure, the values of cell voltage as well as power density are almost equal in the region of low current densities. However, starting from the current density of 50 mA cm^{-2} the difference in performance becomes more significant and keeps growing as the current density increases. In case of the p-PVA membrane the maximum power density of 71 mW cm^{-2} was reached at 200 mA cm^{-2}, whereas performance of the Selemion HSF membrane reached 95% of its maximum. As was previously mentioned, the proton conductivity of the p-PVA membrane is greatly affected by the concentration of H^+ ions (acid), and doping with 1 M H_2SO_4 allowed to achieve the proton conductivity of 3.5×10^{-2} S cm^{-1}, which is close to, but still lower than the conductivity of Selemion HSF membrane in 1 M H_2SO_4 (4.1×10^{-2} S cm^{-1} [25]). Therefore, the larger maximum power density observed for the Selemion HSF (88 mW cm^{-2} at 290 mA cm^{-2}) is quite reasonable, because in the region of higher current densities ohmic resistance within the cell has the biggest impact on a cell voltage. Nonetheless, we believe that the synthesized p-PVA membrane can be a very serious contender in the light of new possibilities for modification and tailoring membranes for specific applications, and due to its unbeatable inexpensiveness in comparison with current commercially available membranes.

4. Conclusions

The results presented above, combined with the data on phosphorylation of PVA available in the literature allowed us to make the following conclusions:

1. Phosphorylation of PVA by hypophosphorous acid at 115–130 °C leads to the formation of mixture of phosphonate and phosphate mono- and diesters. The cross-linking is achieved by formation of interconnected structures.
2. The formation of acid–base complexes in the structure of the synthesized p-PVA membrane, facilitated by the high density of negatively charged oxygen atoms, is believed to provide a strong dependence of proton conductivity on H^+ ions concentration and results in the intrinsic proton conductivity within the range of $1–6 \times 10^{-3}$ S cm^{-1} at 22 °C.
3. The formation of C=C bonds within the p-PVA matrices opens up the possibility for further modifications and tailoring membranes for specific applications by various organic chemistry reactions.
4. The results of membranes testing in a single Fe^{3+}/H_2 redox fuel cell showed a good performance in the region of medium current densities, which allows to suggest their potential use as an effective basis to develop customized membranes for various energy storage applications.

References

[1] D.S. Scott, Int. J. Hydrogen Energy 36 (2011) 9401–9404.
[2] Y. Wang, P. He, H. Zhou, Adv. Energy Mater. 2 (2012) 770–779.
[3] G. Kear, A.A. Shah, F.C. Walsh, Int. J. Energy Res. 36 (2012) 1105–1120.
[4] N. Xu, X. Li, X. Zhao, J.B. Goodenough, K. Huang, Energy Environ. Sci. 4 (2011) 4942–4946.
[5] D.G. Karamanev, V.R. Pupkevich, H. Hojjati, Bio-fuel Cell System. U.S. Patent; US 20100040909 A1, February 18, 2010.
[6] B. Du, Q. Guo, Zh. Qi, L. Mao, R. Pollard, J.F. Elter, in: R.H. Jones, G.J. Thomas (Eds.), Materials for Hydrogen Economy, CRC Press, Boca Raton-London-New York, 2008, pp. 274–285.
[7] T.J. Peckham, Y. Yang, S. Holdcroft, in: D.P. Wilkinson, J. Zhang, R. Hui, J. Fergus, X. Li (Eds.), Proton Exchange Membrane Fuel Cells: Materials, Properties and Performance, CRC Press, Boca Raton-London-New York, 2010, pp. 107–190.
[8] C.-S. Wu, F.-Y. Lin, C.-Y. Chen, P.P. Chu, J. Power Sources 160 (2006) 1204–1210.
[9] A.K. Sahu, G. Selvarani, S.D. Bhat, S. Richumani, P. Sridar, A.K. Shukla, N. Narayanan, A. Banerjee, N. Chandrakumar, J. Membr. Sci. 319 (2008) 298–305.
[10] J. Qiao, T. Hamaya, T. Okada, J. Mater. Chem. 15 (2005) 4414–4423.
[11] J. Qiao, T. Okada, Hydrocarbon Polymer Electrolytes for Fuel Cell Applications, Ibaraki, Japan, 2008.
[12] C.W. Lin, Y.F. Huang, A.M. Kannan, J. Power Sources 171 (2007) 340–347.
[13] C.-C. Shen, J. Joseph, Y.-C. Lin, S.-H. Lin, C.-W. Lin, B.J. Hwang, Desalination 233 (2008) 82–87.
[14] J.-W. Rhim, H.B. Park, Ch.-S. Lee, J.-H. Jun, D.S. Kim, Y.M. Lee, J. Membr. Sci. 238 (2004) 143–151.
[15] Yu.A. Dobrovolsky, A.V. Pisareva, L.S. Leonova, A.I. Karelin, Int. J. Altern. Energy Ecol. 12 (2004) 36–41.
[16] N.A. Shoudhury, S.K. Prashant, S. Pitchumani, P. Sridar, A.K. Shukla, J. Chem. Sci. 121 (2009) 647–654.
[17] V. Pupkevich, V. Glibin, D. Karamanev, Abstracts of 94th Canadian Chemistry Conference and Exhibition, June 5–9, Montreal, Canada (2011) EG2 0692.
[18] M. Suzuki, T. Yoshida, T. Koyama, S. Kobayashi, M. Kimura, K. Hanabusa, H. Shirai, Polymer 41 (2000) 4531–4536.
[19] F. Chen, P. Liu, Macromol. Res. 19 (2011) 883–890.
[20] B.P. Tripathi, A. Saxena, V.K. Shahi, J. Membr. Sci. 318 (2008) 288–297.
[21] V.V. Binsu, R.K. Nagarale, V.K. Shahi, J. Mater. Chem. 15 (2005) 4823–4831.
[22] Z. Jiang, X. Zheng, H. Wu, F. Pan, J. Power Sources 185 (2008) 85–94.
[23] F. Helfferich, Ion Exchange, McGraw Hill, New York, 1962.
[24] M. Banks, J.R. Ebdon, M. Johnson, Polymer 34 (1993) 4547–4551.
[25] V.R. Pupkevich, V.P. Glibin, D.G. Karamanev, J. Solid State Electrochem. 11 (2007) 1429–1434.
[26] R. Balgobin, B. Garcia, D. Karamanev, V. Glibin, Solid State Ionics 181 (2010) 1403–1407.
[27] J. Xi, Z. Wu, X. Qiu, L. Chen, J. Power Sources 166 (2007) 531–536.
[28] V. Pupkevich, V.P. Glibin, D.G. Karamanev, Electrochem. Commun. 9 (2007) 1924–1930.
[29] V.E. Bel'ski, Russ. Chem. Rev. 46 (1977) 828–841.
[30] J. Coates, in: R.A. Meyers (Ed.), Encyclopedia of Analytical Chemistry, John Wiley & Sons Ltd., New York, 2003, pp. 10815–10837.
[31] C.N.R. Rao, Chemical Applications of Infrared Spectroscopy, Academic Press, New York, London, 1963.
[32] J. Goldenson, Appl. Spectrosc. 18 (1964) 155–157.
[33] J. Guan, G.S.-C. Choy, R. Glaser, G.J. Thomas Jr., J. Phys. Chem. 99 (1995) 12054–12062.
[34] M.W. Schmidt, P.N. Truong, M.S. Gordon, J. Am. Chem. Soc. 109 (1987) 5217–5227.
[35] R. Withnall, L. Andrews, J. Phys. Chem. 91 (1987) 784–797.
[36] B.M. Vuano, S.G. Acebal, O. Sala, O. Brieux, O.I. Pieroni, J. Mol. Struct. THEOCHEM 690 (2004) 77–81.
[37] G.H. Li, S.H. Kim, C.G. Cho, Macromol. Res. 14 (2006) 504–509.
[38] A. Heras, N.M. Rodrigez, V.M. Ramos, E. Agullo, Carbohydr. Polym. 44 (2001) 1–8.
[39] E.K. Fields, J. Am. Chem. Soc. 80 (1958) 2358–2362.

[40] L.W. Daasch, D.C. Smith, Anal. Chem. 23 (1951) 853–868.
[41] K. Ohwada, Appl. Spectrosc. 22 (1968) 209–210.
[42] G. Frenking, H. Goetz, F. Marschner, J. Am. Chem. Soc. 100 (1978) 5295–5296.
[43] B.M. Weckhuysen, I.E. Wachs, J. Chem. Soc. Faraday Trans. 92 (1996) 1969–1973.
[44] R.M. Badger, J. Chem. Phys. 3 (1935) 710–714.
[45] V.I. T'ulin, Izvestiya Vouzov: Khimia i Khimitcheskaya Tekhnologia (Commun. Rus. Higher Schools: Chem. Chem. Tech. 34 (1991) 34–38 (in Russian).
[46] T.L. Cottrell, The Strengths of Chemical Bonds, Butterworths Scientific Publications, London, 1954.
[47] E.A. Robinson, Can. J. Chem. 41 (1963) 3021–3033.
[48] R.F. See, J. Chem. Educ. 86 (2009) 1241–1247.
[49] E. Kraka, D. Cremer, Chem. Phys. Chem. 10 (2009) 686–698.
[50] H. Goldwhite, Introduction to Phosphorus Chemistry, Cambridge University Press, Cambridge, 1981.
[51] I.D. Brown, The Chemical Bond in Inorganic Chemistry, The Bond Valence Model, University Press, Oxford, New York, 2002.
[52] G. Lendvay, J. Mol. Struct. THEOCHEM 501–502 (2000) 389–393.
[53] H. Cheng, I. Nicolic-Hughes, J.H. Wang, H. Deng, P.J. O'Brien, L. Wu, Z.-Y. Zhang, D. Herschlag, R. Callender, J. Am. Chem. Soc. 124 (2002) 11295–11306.
[54] A. Iribarren, A. Lopez-Marzo, H. Lemmetyinen, Revista Cubana de Quimica 21 (2009) 3–9.
[55] M. Sander, E. Steininger, J. Mol. Sci. C2 (1968) 57–72.
[56] M. Sander, E. Steininger, J. Mol. Sci. C1 (1967) 91–177.
[57] M. Sander, E. Steininger, J. Mol. Sci. C1 (1967) 7–89.
[58] M. Henry, J.P. Jolivet, J. Livage, in: R. Reisfeld (Ed.), Structure and Bonding, vol. 77, Springer Verlag, Berlin-Heidelberg, 1992, pp. 155–206.
[59] A.L. Allred, E.G. Rochow, J. Inorg. Nucl. Chem. 5 (1958) 264–268.
[60] J.C. Carver, R.C. Gray, D.M. Hercules, J. Am. Chem. Soc. 96 (1974) 6851–6856.
[61] F. Forner, H.M. Badawi, J. Theoret. Comput. Chem. 7 (2008) 1251–1268.
[62] A. Hernandez-Laguna, C.I. Sainz-Diaz, Y.G. Smeyers, J.L.G. de Paz, E. Galvez-Ruano, J. Phys. Chem. 98 (1994) 1109–1116.
[63] L. Li, L. Xu, Y. Wang, Mater. Lett. 57 (2003) 1406–1410.
[64] N. Agmon, Chem. Phys. Lett. 244 (1995) 456.
[65] A.N. Kalinnikov, L.A. Gribov, J. Appl. Spectr. 40 (1984) 414–418.
[66] T.J.R. Weakley, Acta Cryst. B32 (1976) 2889–2890.
[67] S. Furberg, P. Landmark, Acta Chem. Scand. 11 (1957) 1505–1511.
[68] M. O'Keeffe, B. Domenges, J. Phys. Chem. 89 (1985) 2304–2309.
[69] K. Sorensen-Stowell, A.C. Hengee, J. Org. Chem. 70 (2005) 4805–4809.